Annals of R.S.C.B., ISSN:1583-6258, Vol. 25, Issue 3, 2021, Pages. 1858 - 1869
Received 16 February 2021; Accepted 08 March 2021.

# Radiation Effect on MHD Casson Fluid Flow Linearly Porous Stretching Sheet in the Presence Chemical Reaction

**Dr.M.Naga Swapna[1], Dr.P.Anusha[2], Dr.V.Chittaranjandas[3], Dr.K.Srividya[4]**
[1,2] Assistant Professor, Department of Mechanical Engineering, P V P Siddhartha Institute of Technology, Vijayawada.
[3]Professor, R V R & J C College of Engineering, Guntur.
[4]Assosciate Professor, Department of Mechanical Engineering, P V P Siddhartha Institute of Technology, Vijayawada.

**Abstract:**MHD boundary layer fluid flow around a linearly stretching surface in the presence of radiative heat flux, heat generation/absorption, and chemical reaction effects in a permeable surface. The governing equations are converted into ODEs with the help of dimensionless variables and solved by using Runke-KuttaFehlberg method along with shooting technique. The numerical and graphical outcomes are observed and presented via Graphs and table. Also, the Nusselt and Sherwood numbers and skin friction coefficient are illustrated by tables.
**Keywords:** MHD; Casson fluid; Stretching sheet, Radiation, Porous medium.

## Introduction

Generally, fluids are categorized as Newtonian and non-Newtonian. The Newtonian fluids represent the linear correlation that exists between shear stress and shear rate. On the opposite, the nonlinear relation between shear stress and strain is expressed by non-Newtonian fluids. Examples of Newtonian fluids are water, oil etc while Casson, micropolar, power law fluids etc are examples on non-Newtonian fluids. One of the most popular non-Newtonian fluid is Casson fluid. It finds applications in food processing, biological engineering and drilling activities. The flow of Casson fluid in 3D past a penetrable linearly stretchable layer is explained by Mahanta and Shaw [1]. The attribute of thermal radiation is explained by Samrat et al.[2] with the unstable flow of Casson nano fluid past a stretchable surface.The effect of multiple slips on MHD non-Newtonian nano fluid flow past an elongated sheet was studied by Raza et al. [3]. Mukhopadhyay et al.[4] gave detailed behaviour over a stretchable surface of Casson fluid. Nadeem et al.[5] have elucidated the flow of Casson fluid with MHD past an exponential and shrinking layer. Vijaya and Reddy [6] discussed Casson fluid flow past an upward penetrable plate with radiation as well as Soret impact. Krishna et al. [7] elucidate chemically reactive MHD flow of Casson fluid with penetrable stretchable sheet. The recent study of Idowu and Falodun [8] discussed the simultaneous flow of two non-Newtonian fluids by varying viscosity as well as thermal conductivity. In another study of Idowu and Falodun [9] presented discussion on MHD non-Newtonian nano fluid past a slanting plate with thermophoresis. Idowu et al.[10] studied Casson dissipative fluid by varying viscosity alongside thermal conductivity.

Annals of R.S.C.B., ISSN:1583-6258, Vol. 25, Issue 3, 2021, Pages. 1858 - 1869
Received 16 February 2021; Accepted 08 March 2021.

The thermal radiation acts a major role in industrial engineering. It major importance on heat transport process is in design of energy system utilized at a very higher temperature. Examples are missiles, gas turbines, space vehicles, nuclear power plants and satellites. Manglesh and Gorla [11] explored unsteadiness of MHD viscoelastic slip motion with thermal radiation alongside chemically reactive rotating channel. Ullah et al. [12] extensively discussed the unsteadiness of MHD Casson fluid with thermal radiation and situated in a penetrable channel. Bala [13] elucidate Casson fluid attribute with MHD flowing through an exponentially slanting penetrable surface with thermal radiation as well as chemical reaction. Chemical reaction effects on heat alongside mass transport by mixed convection laminar flow in an upward surface with induced magnetic field and radiation is discussed by Ibrahim et.al [14].

Inspired by the literature discussed above to study a steady two-dimensional flow of a viscous, incompressible non-Newtonian MHD Casson nanofluid flow over a nonlinear stretching porous sheet with radiation and chemical reaction. Similarity transformation has been utilized to simplify the governing equations, and the reduced boundary value problems are solved using Runge-kutta Fehelberg method alongside shooting technique.The effects of various flow parameters on velocity, temperature and concentration profiles as well as the skin-friction, Nusselt number and Shear wood number are discussed qualitatively and discussed graphically.

**Formulation of the problem**

The steady two-dimensional flow of viscous incompressible fluids has been considered by us. The flow is taken into account in different fluid activity situations induced by the stretching velocity of the linearly extended sheet $u_w(x) = ax$ where $a$ is a positive constant. Also, $T_w$and $C_w$are the fluid's temperature and concentration near the permeable stretched surface. With constant intensity $Bo$, magnetic field is applied in $y$ direction. In the direction of chemical reaction, thermal radiation and thermophoretic velocity, temperature and concentration are taken into account.

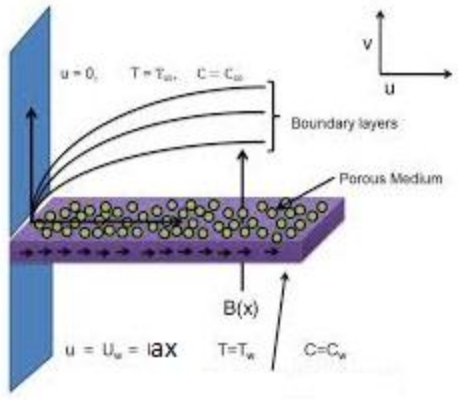


Fig.1 Physical model of the problem

Annals of R.S.C.B., ISSN:1583-6258, Vol. 25, Issue 3, 2021, Pages. 1858 - 1869
Received 16 February 2021; Accepted 08 March 2021.

According to the constitutive equation of Casson fluid as described as follows:

$$\tau_{ij} = \begin{cases} \left(\mu_b + \frac{P_y}{\sqrt{2\pi}}\right) 2e_{ij} & \text{when } \pi > \pi_c \\ \left(\mu_b + \frac{P_y}{\sqrt{2\pi_c}}\right) 2e_{ij} & \text{when } \pi < \pi_c \end{cases} \tag{1}$$

where $P_y$ signifies Casson yield stress expressed as

$$P_y = \frac{\mu_b \sqrt{(2\pi)}}{\beta} \tag{2}$$

$\mu_b$ = plastic dynamic viscosity, $\pi = e_{ij}e_{ij}$ = multiplication of the component of deforming rate with itself and $e_{ij}$ = deformation rate and $\pi_c$ = critical value subject to Casson model. The Casson liquid flow where $\pi > \pi_c$, we have

$$\mu_0 = \mu_b + \frac{P_y}{\sqrt{2\pi}} \tag{3}$$

putting equation (2) into (3), thus kinematic viscosity is subject to plastic dynamic viscosity $\mu_b$, the density $\rho$ and Casson term $\beta$ gives

$$\mu_0 = \frac{\mu_b}{\rho}\left(1 + \frac{1}{\beta}\right) \tag{4}$$

Putting into consideration all the assumptions, the flows equations that govern the model are as follows:

$$\frac{\partial u}{\partial x} + \frac{\partial v}{\partial y} = 0 \tag{5}$$

$$u\frac{\partial u}{\partial x} + v\frac{\partial u}{\partial y} = \left(1 + \frac{1}{\beta}\right)\frac{\partial^2 u}{\partial y^2} - \frac{\sigma B_0^2}{\rho}u - \frac{\nu}{K}u - \lambda\left(u^2\frac{\partial^2 u}{\partial y^2} + v^2\frac{\partial^2 u}{\partial y^2} + 2uv\frac{\partial^2 u}{\partial x \partial y}\right) + \sqrt{2}\nu\Gamma\frac{\partial v}{\partial y}\frac{\partial^2 u}{\partial y^2} \tag{6}$$

$$u\frac{\partial T}{\partial x} + v\frac{\partial T}{\partial y} = \alpha\frac{\partial^2 T}{\partial y^2} - \frac{1}{\rho c_p}\frac{\partial q_r}{\partial y} + \frac{\mu}{\rho c_p}\left(\frac{\partial u}{\partial y}\right)^2 + \frac{\sigma B_0^2 u^2}{\rho c_p} + \frac{Q_0}{\rho c_p}(T - T_\infty) \tag{7}$$

$$u\frac{\partial C}{\partial x} + v\frac{\partial C}{\partial y} = D_B\frac{\partial^2 C}{\partial y^2} - Kr(C - C_\infty) + \frac{D_T}{T_\infty}\frac{\partial^2 T}{\partial y^2} \tag{8}$$

Subject to the boundary conditions are:

$$\begin{aligned} &u(x,0) = u_w = ax,\ \ v(x,0) = -v_w, T = T_w, C = C_w \text{ at } y = 0 \\ &u(x,y) \to 0,\ T \to T_\infty, C \to C_\infty \qquad\qquad \text{as } y \to \infty \end{aligned} \tag{9}$$

Here the horizontal and vertical components of velocity $u$ and $v$ are in directions $x$ and $y$ direction, $\nu$ signifies viscosity, $\beta$ signifies Casson term, $\sigma$ signifies electrical conductivity, $B_0$

Annals of R.S.C.B., ISSN:1583-6258, Vol. 25, Issue 3, 2021, Pages. 1858 - 1869
Received 16 February 2021; Accepted 08 March 2021.

signifies magnetic constant, $\rho$ signifies density, $K$ signifies porosity term, T signifies temperature, $\alpha$ signifies thermal conductivity, $\tau$ signifies heat capacity ratio, $D_B$ signifies mass diffusivity, C signifies concentration, $D_T$ signifies thermophoretic diffusion coefficient, $T_\infty$ signifies ambient temperature, signifies coefficient of viscosity, $Cp$ signifies specific heat, $q_r$ signifies radiative heat flux, $Kr$ signifies chemical reaction term.

The radiative heating flux in the temperature equation is calculated and simplified by the Rosseland approximation, i.e,

$$q_r = -\frac{4\sigma_s}{3k_e}\frac{\partial T^4}{\partial y} \tag{10}$$

From the above, the Stefan-Boltzman constant is $\sigma_s$ and the mean absorption coefficient is $k_e$. Let surmised that the difference in temperature in the flow are sufficiently small so that $T^4$ may be expressed in a linear form by expanding $T^4$ about $T_\infty$ using Taylor series and neglecting higher terms to obtain

$$T^4 \neg\ 4T_\infty^3 T - 3T_\infty^4 \tag{11}$$

Introducing the similarity transformation defined as follows are employed in this study

$$\begin{aligned} &\psi = x\sqrt{av}\, f(\eta), u = ax^n f'(\eta), v = -\sqrt{av}\, f, \eta = \sqrt{\frac{a}{\nu}}y, \\ &\theta(\eta) = \frac{T-T_\infty}{T_w - T_\infty}, \phi(\eta) = \frac{C-C_\infty}{C_w - C_\infty}, T_w = T_\infty + bx, C_w = C_\infty + cx \end{aligned} \tag{12}$$

With respect to equation (12) above, the governing flow equations are simplified to obtain

$$\left(1+\frac{1}{\beta}\right) f''' + ff'' - (f')^2 - \lambda\left(f^2 f''' - 2f\, f'\, f''\right) - \left(M + 1/K\right) f' + We\, f''\, f''' = 0 \tag{13}$$

$$\left(1+\frac{4R}{3}\right)\theta'' + \Pr\left(f\theta' - f'\theta\right) + PrEc\left(f'' + Mf'^2\right) + Q\Pr\theta = 0 \tag{14}$$

$$\phi'' + Sc\left(f\phi' - f'\phi\right) + ScSr\theta'' - ScKr\phi = 0 \tag{15}$$

with the constraints:

$$\begin{aligned} &f(0) = S,\ f'(0) = 1, \theta(0) = 1, \phi(0) = 1 \\ &f'(\infty) = 1, \theta(\infty) = 0, \phi(\infty) = 0 \end{aligned} \tag{16}$$

The engineering curiosity are skin friction $(C_f)$, local Nusselt $(Nu)$ and Sherwood $(Sh)$ defined as follows:

$$C_f = \frac{\tau_w}{\rho u_w^2},\ Nu = \frac{xq_w}{K(T_w - T_\infty)},\ Sh = \frac{xq_m}{D_B(C_w - C_\infty)}$$

and $\tau_w$ signifies wall shear stress, $q_w$ signifies heat flux while $q_m$ signifies mass flux. They are

$$\tau_w = \mu_B\left(1+\frac{1}{\beta}\right)\left(\frac{\partial u}{\partial y}\right)_{y=0},\ q_w = -K\left(\frac{\partial T}{\partial y}\right)_{y=0},\ q_m = -D_B\left(\frac{\partial C}{\partial y}\right)_{y=0}$$

Employing equation on the above to obtain

Annals of R.S.C.B., ISSN:1583-6258, Vol. 25, Issue 3, 2021, Pages. 1858 - 1869
Received 16 February 2021; Accepted 08 March 2021.

$$Re_x^{\frac{1}{2}} C_f = \left(1+\frac{1}{\beta}\right) f''(0),\ Re_x^{\frac{1}{2}} Nu = -\theta'(0),\ Re_x^{\frac{1}{2}} Sh = -\phi(0)$$

**Numerical approach**

The converted nonlinear differential Equations (13)–(15) with the boundary conditions (16) are elucidated by Runge-KuttaFehlberg method along with shooting technique. This method has been proven to be adequate and gives accurate results for the boundary layer equations.

**Results and Discussion**

This section explains the outcomes of the results from solving equation (13)-(15) subject to (16) numerically. To describe the physics of the problem, results are presented in graphs. Figure 2 portrays the behaviour of the imposed magnetic term (M) on the velocity plot. An increment in the value of M as shown in Figure 3 declines the velocity plot. Practically, imposing the magnetism in the flow direction of an electrically conducting fluid such as Casson produces Lorentz force. This force has the tendency to drag the Casson flow by decreasing its velocity. hence, the fluid velocity alongside its momentum layer thickness is declined. This implies that, increase in M added more strength to the Lorentz force.

Figure 3 portrays the effect of porosity term (K) on the velocity plot. It is noticed that an incremental value of K leads to degeneration in the velocity plot as well as the momentum layer thickness. Physically, a hike in K makes very hard for the fluids particles to move freely and hereby resist the velocity gradually. Figure 4 presents the effect of Maxwell ($\lambda$) on the velocity profiles. It is noticed that an incremental value of $\lambda$ leads to degeneration in the velocity plot as well as the momentum layer thickness. Physically, a hike in $\lambda$ makes very hard for the fluids particles to move freely and hereby resist the velocity gradually.Figure 5 depict the behavior of Williamson parameter (We) on the velocity field. It is observed that the velocity decreases with an incresing the Williamson parameter.

Figure 6 represents the impact of the Prandtl number (Pr) on the temperature plot. A less fluid temperature alongside thermal layer thickness is noticeable for a large Pr. Hence, when $Pr << 1$, it implies thermal diffusivity controls the flow behavior while implies momentum diffusivity controls the flow behavior. Therefore, is useful in controlling cooling rate of a conducting fluid electrically. In this study, there exist a wall temperature and free stream temperature which gives rise to $T_w - T_\infty$ along with thermal boundary layer thickness.

Figure 7 portrays the role of thermal radiation $(R)$ on the temperature plot. A large value of R is observed to hike the temperature plot. This implies an enhancement in the thermal layer thickness. Physically, the thermal radiation helps to boost the thermal situation of the fluid environment. Hence, increasing R helps to boost the heat on the fluid and hereby lead to enhancement in the temperature of the fluid. Figure 8 shows the effect of Eckert number $(Ec)$ on the temperature plot. An increment in the value of $Ec$ from $0.1$ to $0.4$ is observed to degenerate

Annals of R.S.C.B., ISSN:1583-6258, Vol. 25, Issue 3, 2021, Pages. 1858 - 1869
Received 16 February 2021; Accepted 08 March 2021.

the temperature plot alongside the thermal layer thickness. Ec portray the flow kinetic energy and its associated enthalpy. The viscous dissipation term (Eckert number) hike heat energy to the fluid environment. Physically, Eckert number and thermal radiation in a fluid flow increase the rate of heat transfer.

Figure 9 depicts the effect of the heat source parameter (Q) on the temperature profiles. A large value of Q is observed to increases the temperature increases as well as the bounary layer thickness. Figure 10 shows the impact of the chemical reaction term $(Kr)$ on the concentration plot. An incremental value of Kr is observed to degenerate the concentration plot. Physically, it indicate a destructive chemical reaction. Figure11 presents the impact of varying the Soret number (n) on the concentration profiles.It is observed that the concetration increases with an increasing the Soret number due mass diffusivity. Figure 12 represents the effect of the Schmidt numebr number (Sc) on the concentration plot. An increment in Sc is observed in figure 12 to degenerate the concentration plot.

Figure 14 portrays the impact of the Casson $(\beta)$ electrically conducting fluid on the velocity plot. A large value of $\beta$ is detected to degenerate the velocity plot from 1 to 4. This indicates that the density alongside momentum layer thickness declines for a large value of $\beta$. Experimentally, when $\beta \to \infty$ it is detected that the behaviour of $\beta$ is equivalent to a Newtonian behaviour. Physically, the Casson fluid possesses a plastic dynamic viscosity originates a resistance to the fluid flow by decreasing the velocity plot.

Table 1 shows the impact of various flow parameters on the engineering interest. All pertinent flow parameters were found to have great effect on the skin friction, Nusselt and Sherwood number.

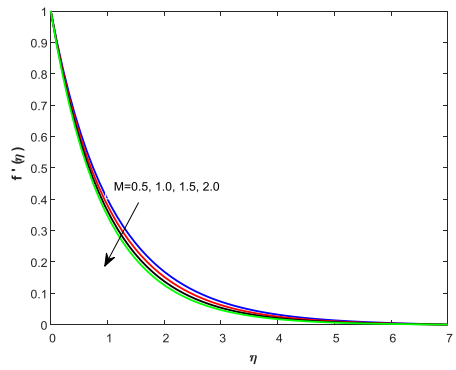


Fig.2. Velocity profiles for different values of M.

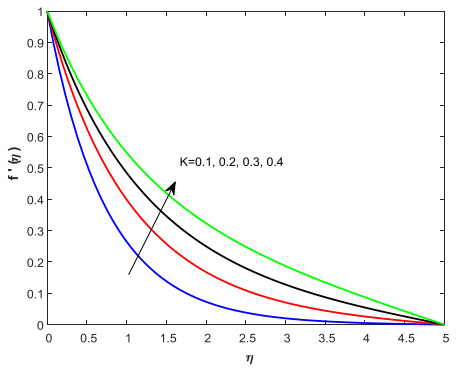


Fig.3. Velocity profiles for different values of K.

Annals of R.S.C.B., ISSN:1583-6258, Vol. 25, Issue 3, 2021, Pages. 1858 - 1869
Received 16 February 2021; Accepted 08 March 2021.

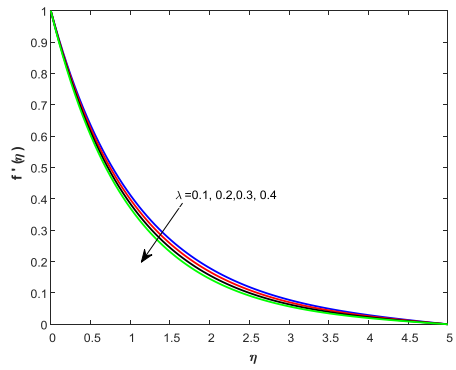


Fig.4. Velocity profiles for different values of λ.

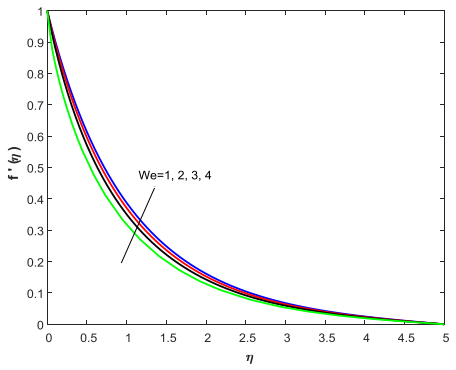


Fig.5. Velocity profiles for different values of We.

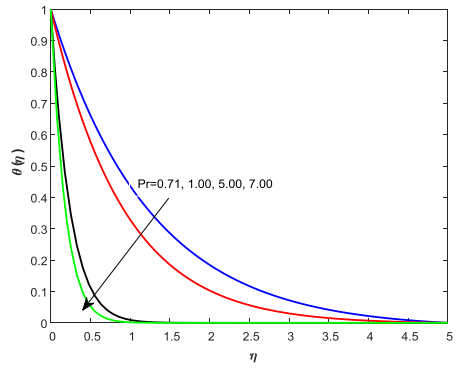


Fig.6. Temperature profiles for different values of Pr.

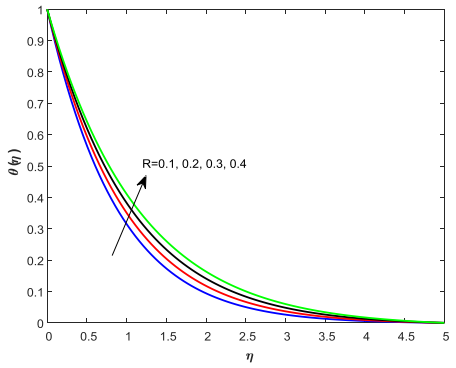


Fig.7. Temperature profiles for different values of R.

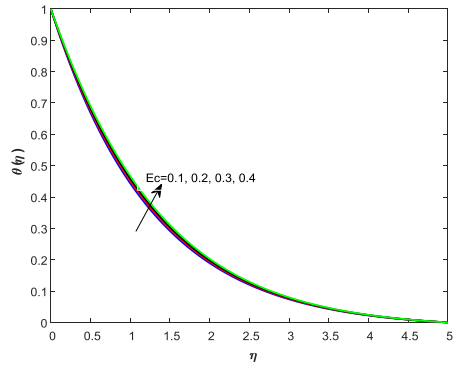


Fig.8. Temperature profiles for different values of Ec.

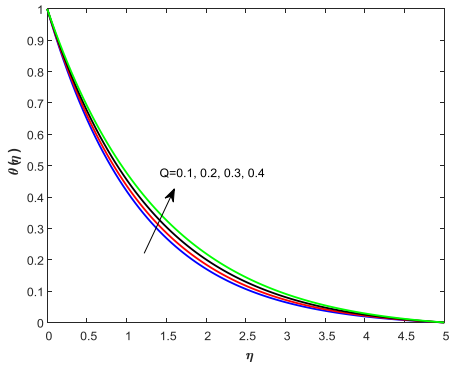


Fig.9. Temperature profiles for different values of Q.

Annals of R.S.C.B., ISSN:1583-6258, Vol. 25, Issue 3, 2021, Pages. 1858 - 1869
Received 16 February 2021; Accepted 08 March 2021.

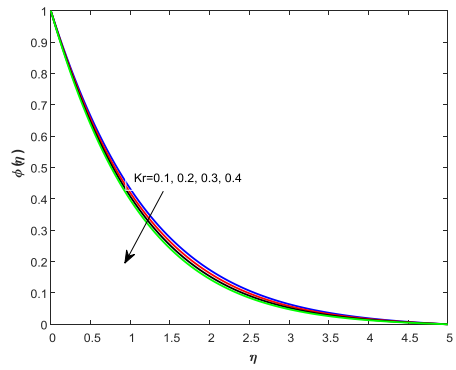


Fig.10. Concentration profiles for different values of Kr.

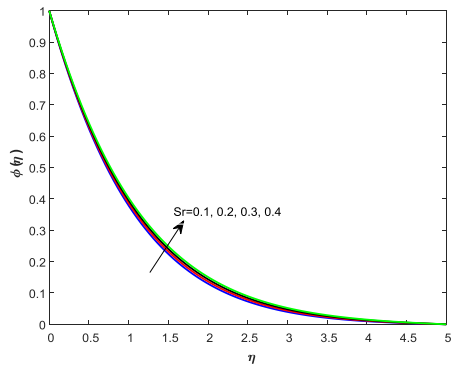


Fig.11. Concentration profiles for different values of Sr.

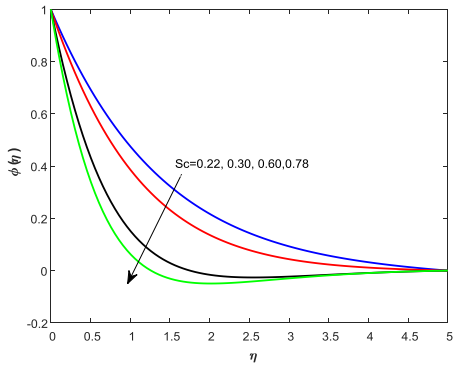


Fig.12. Concentration profiles for different values of Sc

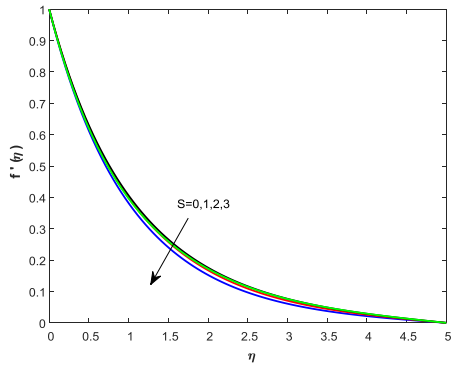


Fig.13. Velocity profiles for different values of S

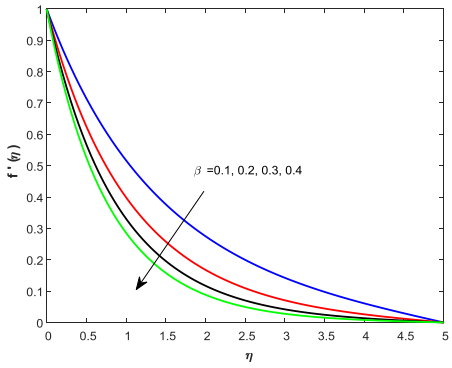


Fig.14. Velocity profiles for different values of β

Table-1

| M | K | L | B | We | Pr | R | Ec | Q | Kr | Sr | Sc | S | $-f''(0)$ | $-\theta'(0)$ | $-\phi'(0)$ |
|---|---|---|---|---|---|---|---|---|---|---|---|---|---|---|---|
| 0.5 | 0.2 | 0.2 | 0.2 | 0.2 | 0.71 | 0.5 | 0.001 | 0.2 | 0.5 | 0.2 | 0.3 | 1 | 0.964723 | 0.784940 | 0.862801 |
| 1 | | | | | | | | | | | | | 1.013387 | 0.794945 | 0.872578 |

Annals of R.S.C.B., ISSN:1583-6258, Vol. 25, Issue 3, 2021, Pages. 1858 - 1869
Received 16 February 2021; Accepted 08 March 2021.

| | | | | | | | | | | | | | | | |
|---|---|---|---|---|---|---|---|---|---|---|---|---|---|---|---|
| 1.5 | | | | | | | | | | | | | 1.059556 | 0.805669 | 0.883628 |
| 0.5 | 0.1 | 0.2 | 0.2 | 0.2 | 0.71 | 0.5 | 0.001 | 0.2 | 0.5 | 0.2 | 0.3 | 1 | 0.659391 | 0.750992 | 0.820321 |
| | 0.2 | | | | | | | | | | | | 0.777937 | 0.826915 | 0.895492 |
| | 0.3 | | | | | | | | | | | | 0.965054 | 0.868085 | 0.948321 |
| | 0.4 | | | | | | | | | | | | 1.370939 | 0.896015 | 0.991423 |
| 0.5 | 0.2 | 0.1 | 0.2 | 0.2 | 0.71 | 0.5 | 0.001 | 0.2 | 0.5 | 0.2 | 0.3 | 1 | 0.932973 | 0.812506 | 0.879438 |
| | | 0.2 | | | | | | | | | | | 0.965054 | 0.819809 | 0.887445 |
| | | 0.3 | | | | | | | | | | | 0.998579 | 0.826915 | 0.895492 |
| | | 0.4 | | | | | | | | | | | 1.033620 | 0.833816 | 0.903566 |
| 0.5 | 0.2 | 0.2 | 0.1 | 0.2 | 0.71 | 0.5 | 0.001 | 0.2 | 0.5 | 0.2 | 0.3 | 1 | 0.932973 | 0.812506 | 0.879438 |
| | | | 0.2 | | | | | | | | | | 0.965054 | 0.819809 | 0.887445 |
| | | | 0.3 | | | | | | | | | | 0.998579 | 0.826915 | 0.895492 |
| | | | 0.4 | | | | | | | | | | 1.033620 | 0.833816 | 0.903566 |
| 0.5 | 0.2 | 0.2 | 0.2 | 0.1 | 0.71 | 0.5 | 0.001 | 0.2 | 0.5 | 0.2 | 0.3 | 1 | 1.018160 | 0.769299 | 0.844399 |
| | | | | 0.2 | | | | | | | | | 1.113553 | 0.797790 | 0.867995 |
| | | | | 0.3 | | | | | | | | | 1.300727 | 0.810917 | 0.879969 |
| | | | | 0.4 | | | | | | | | | 1.901165 | 0.820583 | 0.889197 |
| 0.5 | 0.2 | 0.2 | 0.2 | 0.2 | 0.71 | 0.5 | 0.001 | 0.2 | 0.5 | 0.2 | 0.3 | 1 | 0.965054 | 0.826915 | 0.632210 |
| | | | | | 1 | | | | | | | | 0.965054 | 1.086954 | 0.710247 |
| | | | | | 5 | | | | | | | | 0.965054 | 4.007342 | 0.880836 |

Annals of R.S.C.B., ISSN:1583-6258, Vol. 25, Issue 3, 2021, Pages. 1858 - 1869
Received 16 February 2021; Accepted 08 March 2021.

| | | | | | | | | | | | | | | | |
|---|---|---|---|---|---|---|---|---|---|---|---|---|---|---|---|
| | | | | | 7 | | | | | | | | 0.965054 | 5.319734 | 0.895492 |
| 0.5 | 0.2 | 0.2 | 0.2 | 0.2 | 0.71 | 0.1 | 0.001 | 0.2 | 0.5 | 0.2 | 0.3 | 1 | 0.965054 | 0.883261 | 0.878659 |
| | | | | | | 0.2 | | | | | | | 0.965054 | 0.949688 | 0.884109 |
| | | | | | | 0.3 | | | | | | | 0.965054 | 1.029048 | 0.888585 |
| | | | | | | 0.4 | | | | | | | 0.965054 | 1.125411 | 0.892324 |
| 0.5 | 0.2 | 0.2 | 0.2 | 0.2 | 0.71 | 0.2 | 0.1 | 0.2 | 0.5 | 0.2 | 0.3 | 1 | 0.965054 | 0.717804 | 0.897040 |
| | | | | | | | 0.2 | | | | | | 0.965054 | 0.745150 | 0.898604 |
| | | | | | | | 0.3 | | | | | | 0.965054 | 0.772495 | 0.900168 |
| | | | | | | | 0.4 | | | | | | 0.965054 | 0.799841 | 0.901731 |
| 0.5 | 0.2 | 0.2 | 0.2 | 0.2 | 0.71 | 0.2 | 0.001 | 0.1 | 0.5 | 0.2 | 0.3 | 1 | 0.965054 | 0.740640 | 0.893336 |
| | | | | | | | | 0.2 | | | | | 0.965054 | 0.785586 | 0.895492 |
| | | | | | | | | 0.3 | | | | | 0.965054 | 0.826915 | 0.897811 |
| | | | | | | | | 0.4 | | | | | 0.965054 | 0.865294 | 0.900329 |
| 0.5 | 0.2 | 0.2 | 0.2 | 0.2 | 0.71 | 0.2 | 0.001 | 0.2 | 0.1 | 0.2 | 0.3 | 1 | 0.965054 | 0.826915 | 0.794225 |
| | | | | | | | | | 0.2 | | | | 0.965054 | 0.826915 | 0.821370 |
| | | | | | | | | | 0.3 | | | | 0.965054 | 0.826915 | 0.847192 |
| | | | | | | | | | 0.4 | | | | 0.965054 | 0.826915 | 0.871854 |
| 0.5 | 0.2 | 0.2 | 0.2 | 0.2 | 0.71 | 0.2 | 0.001 | 0.2 | 0.5 | 0.1 | 0.3 | 1 | 0.965054 | 0.826915 | 0.860042 |
| | | | | | | | | | | 0.2 | | | 0.965054 | 0.826915 | 0.877767 |
| | | | | | | | | | | 0.3 | | | 0.965054 | 0.826915 | 0.895492 |

Annals of R.S.C.B., ISSN:1583-6258, Vol. 25, Issue 3, 2021, Pages. 1858 - 1869
Received 16 February 2021; Accepted 08 March 2021.

| | | | | | | | | | | | | | | | |
|---|---|---|---|---|---|---|---|---|---|---|---|---|---|---|---|
| | | | | | | | | | | 0.4 | | | 0.965054 | 0.826915 | 0.913217 |
| 0.5 | 0.2 | 0.2 | 0.2 | 0.2 | 0.71 | 0.2 | 0.001 | 0.2 | 0.5 | 0.2 | 0.1 | 1 | 0.965054 | 0.826915 | 0.718195 |
| | | | | | | | | | | | 0.2 | | 0.965054 | 0.826915 | 0.895492 |
| | | | | | | | | | | | 0.3 | | 0.965054 | 0.826915 | 1.512335 |
| | | | | | | | | | | | 0.4 | | 0.965054 | 0.826915 | 1.856587 |
| 0.5 | 0.2 | 0.2 | 0.2 | 0.2 | 0.71 | 0.2 | 0.001 | 0.2 | 0.5 | 0.2 | 0.2 | 0 | 0.955964 | 0.504281 | 0.694078 |
| | | | | | | | | | | | | 1 | 0.965054 | 0.826915 | 0.895492 |
| | | | | | | | | | | | | 2 | 0.997637 | 1.186765 | 1.118261 |
| | | | | | | | | | | | | 3 | 1.004992 | 1.561096 | 1.348674 |

**References**

[1] G Mahanta, S Shaw. 3D Casson fluid flow past a porous linearly stretching sheet with convective boundary condition, *Alexandria Engineering Journal* 2015; 54, 653–659.

[2] S P Samrat, CSulochana, G PAshwinkuma., Impact of Thermal Radiation on an Unsteady CassonNanofluid Flow Over a Stretching Surface, *International Journal of Applied and Computational Mathematics* 2019, 5:31 https://doi.org/10.1007/s40819-019-0606-2

[3] RazaJawad, MushayydhaFarooq, FatehMebarek-oudina, B. Mahanthesh. Multiple slip effects on MHD non-Newtonian nanofluid flow over a nonlinear permeable elongated sheet, Multidiscipline Modeling in Materials and Structures 2019; 15(5), 913-931.

[4] Swati Mukhopadhyay, PrativaRanjan De, Krishnendu Bhattacharyya, G.C. Layek.Casson fluid flow over an unsteady stretching surface,*Ain Shams Engineering Journal* 2013;4, 933–938.

[5] S Nadeem, RizwanUlHaq, C Lee. MHD flow of a Casson fluid over an exponentially shrinking sheet, *ScientiaIranica B* 2012; 19 (6), 1550–1553

[6] K Vijaya, G V R Reddy.Magnetohydrodynamic casson fluid flow over a vertical porous plate in the presence of radiation, soret and chemical reaction effects, *Journal of Nanofluids*, 2019; 8(6), 1240-1248.

[7] Y H Krishna, G V R Reddy, O D Makinde. Chemical reaction effect on MHD flow of casson fluid with porous stretching sheet, *Defect and Diffusion Forum* ,2018; 389, 100-109.

Annals of R.S.C.B., ISSN:1583-6258, Vol. 25, Issue 3, 2021, Pages. 1858 - 1869
Received 16 February 2021; Accepted 08 March 2021.

[8] A S Idowu, B O Falodun.Variable thermal conductivity and viscosity effects on non-Newtonian fluids flow through a vertical porous plate under Soret-Dufour influence, *Mathematics and Computers in Simulation* , 2020; 177, 358–384.

[9] S Idowu and B OFalodun. Effects of thermophoresis, Soret-Dufour on heat and mass transfer flow of magnetohydrodynamics non-Newtonian nanofluid over an inclined plate, *Arab Journal of Basic and Applied Sciences*, 2020, 27(1), 149-165..

[10] S Idowu Amos, T MojeedAkolade , Jos U. AbubakarandBidemi O Falodun. MHD free convective heat and mass transfer flow of dissipative Casson fluid with variable viscosity and thermal conductivity effects, *Journal of Taibah University for Science*, 2020, 14(1) 851-862, DOI: 10.1080/16583655.2020.1781431.

[11] MangleshAarti and M. G. Gorla. The Effects of Thermal Radiation, Chemical Reaction and Rotation on Unsteady MHD Viscoelastic Slip Flow, *Global Journal of Science Frontier Research Mathematics and Decision Sciences*,2012; 12, 1-15.

[12] Ullah,K Bhattacharyya, S Shafie, I Khan. Unsteady MHD Mixed Convection Slip FlowofCasson Fluid over Nonlinearly Stretching Sheet Embedded in a Porous Medium with Chemical Reaction, Thermal Radiation, Heat Generation/ Absorption and Convective Boundary Conditions. *PLoS ONE,* 2016, 11(10). doi:10.1371/journal.pone.0165348

[13] PBalaAnki Reddy, Magnetohydrodynamic flow of a Casson fluid over an exponentially inclined permeable stretching surface with thermal radiation and chemical reaction, *Ain Shams Engineering Journal* 2016;7, 593–602.

[14] S M Ibrahim, F Mabood, K Suneetha, G Lorenzini.Effects of chemical reaction on combined heat and mass transfer by laminar mixed convection flow from vertical surface with induced magnetic field and radiation, *Journal of Engineering Thermophysics*,2017;26(2), 234-255.